Journal of Ethnopharmacology 309 (2023) 116377

Contents lists available at ScienceDirect

Journal of Ethnopharmacology

journal homepage: www.elsevier.com/locate/jethpharm

The potential antidiabetic properties of green and purple tea [*Camellia sinensis* (L.) O Kuntze], purple tea ellagitannins, and urolithins

M. Tolmie [a,*], M.J. Bester [b], J.C. Serem [b], M. Nell [c], Z. Apostolides [a]

[a] Department of Biochemistry, Genetics and Microbiology at the University of Pretoria, Pretoria, South Africa
[b] Department of Anatomy at the University of Pretoria, Pretoria, South Africa
[c] Department of Pharmacology at the University of Pretoria, Pretoria, South Africa

ARTICLE INFO

Keywords:
Type 2 diabetes
Traditional medicine
Camellia sinensis
α-glucosidase inhibition
Cellular lipid accumulation
Cellular glucose uptake

ABSTRACT

Ethnopharmacological relevance: Tea (*Camellia sinensis*) has been consumed for centuries as traditional medicine for various diseases, including diabetes. The mechanism of action of many traditional medicines, including tea, often requires elucidation. Purple tea is a natural mutant of *Camellia sinensis,* grown in China and Kenya, and is rich in anthocyanins and ellagitannins.

Aim of the study: Here we aimed to determine whether commercial green and purple teas are a source of ellagitannins and whether green and purple teas, purple tea ellagitannins and their metabolites urolithins have antidiabetic activity.

Materials and methods: Targeted UPLC-MS/MS was employed to quantify the ellagitannins corilagin, strictinin and tellimagrandin I, in commercial teas. The inhibitory effect of commercial green and purple teas and purple tea ellagitannins was evaluated on α-glucosidase and α-amylase. The bioavailable urolithins were then investigated for additional antidiabetic effects, by evaluating their effect on cellular glucose uptake and lipid accumulation.

Results: Corilagin, strictinin and tellimagrandin I (ellagitannins) were identified as potent inhibitors of α-amylase and α-glucosidase, with K_i values significantly lower ($p < 0.05$) than acarbose. Commercial green-purple teas were identified as ellagitannin sources, with especially high concentrations of corilagin. These commercial purple teas, containing ellagitannins, were identified as potent α-glucosidase inhibitors with IC_{50} values significantly lower ($p < 0.05$) than green teas and acarbose. Urolithin A and urolithin B were as effective ($p > 0.05$) as metformin in increasing glucose uptake in adipocytes, muscle cells and hepatocytes. In addition, similar ($p > 0.05$) to metformin, both urolithin A and urolithin B reduced lipid accumulation in adipocytes and hepatocytes.

Conclusions: This study identified green-purple teas as an affordable widely available natural source with antidiabetic properties. Furthermore, additional antidiabetic effects of purple tea ellagitannins (corilagin, strictinin and tellimagrandin I) and urolithins were identified.

1. Introduction

Diabetes mellitus is one of the greatest health challenges of the 21st century (Sun et al., 2022). It is a chronic metabolic disorder associated with hyperglycaemia, that affects carbohydrate, lipid and protein metabolism, and ultimately leads to a series of micro- and macrovascular complications (Proença et al., 2017). The global diabetes prevalence (20–79-year-olds) in 2021 was estimated to be 10.5% (536.6 million people) (Sun et al., 2022), and the overwhelming majority (90%) of people have type 2 diabetes (T2DM) (Sun et al., 2022). T2DM is characterised by relative insulin deficiency caused by pancreatic β-cell dysfunction and insulin resistance in target organs. Obesity and lack of physical exercise are factors primarily associated with T2DM and can often lead to other complications such as non-alcoholic fatty liver disease (NAFLD) and metabolic syndrome. NAFLD is characterised by hepatic fat accumulation (Loomba and Sanyal, 2013), while metabolic syndrome is a constellation of abnormalities generally considered to include obesity, hyperglycaemia, dyslipidaemia, and hypertension, which together increase the risk of diabetes and cardiovascular disease (Haffner, 2006). A strong association between NAFLD, metabolic syndrome and T2DM has been identified, where more than 70% of patients

* Corresponding author. Department of Biochemistry, Genetics and Microbiology, University of Pretoria, Private Bag X20, Hatfield, Pretoria, 0028, South Africa.
E-mail addresses: morne.tolmie@gmail.com (M. Tolmie), megan.bester@up.ac.za (M.J. Bester), june.serem@up.ac.za (J.C. Serem), margo.nell@up.ac.za (M. Nell), zeno.apostolides@up.ac.za (Z. Apostolides).

https://doi.org/10.1016/j.jep.2023.116377
Received 27 February 2023; Accepted 7 March 2023
Available online 11 March 2023
0378-8741/© 2023 The Authors. Published by Elsevier B.V. This is an open access article under the CC BY-NC-ND license (http://creativecommons.org/licenses/by-nc-nd/4.0/).

List of compounds studied

Corilagin (CAS 23094-69-1)
Strictinin (CAS 517-46-4)
Tellimagrandin I (CAS 79786-08-6)
Urolithin A (CAS 1143-70-0)
Urolithin B (CAS 1139-83-9)

Abbreviations

2FVJ	Peroxisome proliferator-activated gamma
2-NBDG	2-Deoxy-2-[(7-nitro-2,1,3-benzoxadiazol-4-yl)amino]-D-glucose
2WR6	Retinol-binding protein
3L4Y	α-Glucosidase
3EKN	Insulin receptor precursor
4A5S	Dipeptidyl peptidase
4GQR	α-Amylase
4GE6	Tyrosine-protein phosphatase
4K1L	Corticosteroid dehydrogenase
4PHU	Fatty acid receptor 1
ABS –	Allosteric binding site
DIADB –	Diabetes database
DMEM	Dulbecco's Modified Eagle Medium
DMSO –	Dimethylsulfoxide
DNSA	3,5–Dinitrosalicylic acid
FCS –	Foetal Calf Serum
GIT –	Gastrointestinal tract
IC_{50} –	Half maximal inhibitory concentration
K_i –	Inhibition constant
K_m –	Michaelis constant
V_{max}	Maximum enzyme velocity
NAFLD	Non-alcoholic fatty liver disease
OA –	Oleic acid
OBS –	Orthosteric binding site
ORO –	Oil Red O
pNPG	p-Nitrophenyl-α-D-glucopyranoside
SMILES	Simplified Molecular-Input Line-Entry System
SRB	Sulforhodamine B
T2DM –	Type 2 diabetes
TCA –	Trichloroacetic acid
UPLC-MS/MS –	Ultra High Precision Tandem Mass Spectrometry
VSW	Virtual Screening Workflow
XP –	Extra precision

with T2DM have NAFLD (Tilg et al., 2017), while studies suggest that individuals with metabolic syndrome are 5 times more likely to develop T2DM (Regufe et al., 2020). Since T2DM is a multifactorial disease, therapy often requires several drugs with different mechanisms of action that either regulate insulin secretion, glucose and/or lipid metabolism as illustrated by the 18 diabetes targets on the Diabetes Database (DIADB) (Sánchez-Pérez et al., 2015). The therapeutic benefits of most antidiabetic drugs are often limited by side effects and cost. Consequently, there is a need for new drugs that have multiple T2DM targets, fewer side effects and are affordable. The first level of treatment is the control of postprandial hyperglycaemia, with some of the most common drug targets being α-amylase and α-glucosidase found in the gastrointestinal tract (GIT) mucosa. Bioaccessibility is an important consideration when evaluating systemic effects on additional targets found in hepatic, muscle, and adipose tissue.

Plants, including *Camellia sinensis* (tea), have been used as traditional medicines for centuries. In China (Sun et al., 2021), India (Modak et al., 2007), and various other Eastern (Ediriweera and Ratnasooriya, 2009) and African countries (Barkaoui et al., 2017; Mahomoodally et al., 2016; Rachid et al., 2012) tea has specifically been used as traditional medicine for diabetes. Tea is one of the most widely consumed beverages in the world and offers a plethora of health benefits, such as antioxidant, anticancer, anti-cardiovascular and antidiabetic activities (Yu et al., 2020). However, the mechanism of action of many traditional medicines, including tea, often needs elucidation or further clarification to enhance therapeutic effects and decrease adverse reactions. Purple teas are derived from *Camellia sinensis,* but unlike green, white, yellow, oolong or black tea, purple teas do not originate from a manufacturing process but are distinct cultivars (Khan et al., 2018). Purple tea cultivars have been identified and commercialised in China, Japan (Sun Rouge) and Kenya (TRFK 306/1). Compared to normal tea, purple teas have high levels of anthocyanins (135-fold) (Khan et al., 2018), anthocyanidins (3.5-fold) (Khan et al., 2018) and proanthocyanidins (3-fold) (Lin et al., 2022). Green, dark, yellow and white tea have been identified as sources of ellagitannins (Yang and Tomas-Barberan, 2019). Ellagitannins are hydrolysable high molecular weight tannins, that are bioavailable but have limited bioaccessibility (Espin et al., 2007), and are metabolised by the colonic microbiota to form urolithin A and urolithin B (Espin et al., 2007; Villalba et al., 2019). Urolithins reach systemic circulation at considerable concentrations and are the main urinary and plasma biomarkers for ellagitannin consumption (Yang and Tomas-Barberan, 2019). Yang and Tomas-Barberan (2019) showed that urolithins were detected in human urine after consumption of teas rich in ellagitannins. Ellagitannins and urolithins have been reported to have many beneficial biological activities such as anticancer, antidiabetic, anti-inflammatory, antioxidant, anti-SARS CoV-2 and cardioprotective properties (Loschwitz et al., 2021; Villalba et al., 2019; Zhang et al., 2021). Ellagitannin daily intake is generally low and has been estimated at approximately 5 mg/day for Western diets, with major contributors being red berries (Villalba et al., 2019). Given the significant seasonality of the production of these fruits, exposure to ellagitannins is variable throughout the year (Villalba et al., 2019), and unavailable in some regions in the world such as Africa, where the prevalence of T2DM is increasing at an alarming rate (Sun et al., 2022). Various studies have identified *Camellia sinensis* as a source of ellagitannins (Yang and Tomas-Barberan, 2019), and tea is affordable, available globally and year-round.

This study aimed to determine whether commercial green and purple teas are a source of ellagitannins and whether these teas have antidiabetic activity. This included the *in silico* and *in vitro* evaluation of α-glucosidase and α-amylase inhibition of green and purple teas and ellagitannins, as well as the effects of urolithins on glucose uptake, and lipid accumulation in diabetic target cell lines. The main hypothesis was that purple teas and ellagitannins will have antidiabetic activity through the inhibition of α-amylase and α-glucosidase, while urolithins will stimulate cellular glucose uptake and reduce lipid accumulation in adipocytes and hepatocytes.

2. Materials and methods

2.1. Materials

Six popular commercial green teas were bought from local supermarkets, these were Dilmah Pure Green Tea, Eve's Special Select Green Tea, Five Roses Perfectly Pure Green Tea, Livewell Green Tea, Tetley Pure Green Tea and Twining's Pure Green Tea. Purple tea variants were imported from a tea shop based in the United Kingdom, Curious Tea (https://www.curioustea.com). The purple teas were black-purple teas (Dian Hong Feng Qing Ye Sheng Purple Tea, Dian Hong De Hong Ye Sheng Purple Tea, Dian Hong Jing Mai Purple Needle Tea), pu-erh

purple tea (Zi Ya Purple Bud), and green-purple tea (Tokunoshima Sun Rouge Purple Tea [Japan], Tumoi Nandi Hills Purple Tea [Kenya]). One purple tea sample, Finlays Purple Tea, was kindly donated by Mr Richard Mose from James Finlays Kenya. The ellagitannins, strictinin and tellimagrandin I, were obtained from Nacalai Tesque Co (Kyoto, KY, JPN). The following reagents were obtained from Sigma-Aldrich Co (St. Louis, MO, USA): 3,5–dinitrosalicylic acid (DNSA), α-glucosidase from *Saccharomyces cerevisiae* (EC 3.2.1.20), acarbose, corilagin, dexamethasone, glucose-free media, isobutylmethylxanthine, maltose monohydrate, metformin, Oil Red O (ORO), oleic acid (OA), p-nitrophenol, p-nitrophenyl-α-D-glucopyranoside (pNPG), porcine pancreatic α-amylase (EC 3.2.1.1), potato starch, rosiglitazone, sulforhodamine B (SRB), urolithin A and urolithin B. Mouse 3T3-L1 fibroblasts, human HepG2 hepatoma and mouse C2C12 myoblasts were obtained from the American Type Culture Collection (ATCC) (Manassas, VA, USA). 2-Deoxy-2-[(7-nitro-2,1,3-benzoxadiazol-4-yl)amino]-D-glucose (2-NBDG) was purchased from Thermofisher Co (Waltham, MA, USA). Dulbecco's modified Eagle's medium (DMEM) and foetal calf serum (FCS) were purchased from Sepsci (Johannesburg, RSA) and Biocom (Pretoria, RSA) respectively.

2.2. In silico docking

A literature review was conducted, using Google Scholar and ScienceDirect, to identify ellagitannins found in tea. The following search terms were used: "ellagitannins" and, "tea" or "*Camellia sinensis*". The FoodDB database (https://foodb.ca) was also consulted.

Then the simplified molecular-input line-entry system (SMILES) notations of each ellagitannin were obtained from PubChem. The two-dimensional structures were drawn with ChemDraw (2020) if the compound was not found in PubChem, and exported as the representative SMILES notation.

The SMILES notation of the identified ellagitannins and urolithins was imported to Maestro (Schrodinger LLC, 2021) to prepare the ligands. The LigPrep function (default settings) was used to prepare the three-dimensional structure of each ligand. Antidiabetic target enzymes were identified on DIA-DB (Sánchez-Pérez et al., 2015). The crystal structures of nine antidiabetic target enzymes (PDB entries: 2WR6, 3EKN, 3L4Y, 4A56, 4GQR, 4GE6, 4K1L, 4PHU, and 2FVJ) were obtained from the Protein Data Bank (PDB) and imported to Maestro (Schrodinger LLC, 2021). The proteins were prepared using the protein preparation wizard. All the cofactors and water molecules (not within the active site) were removed, and the hydrogen bonding was optimised before energy minimisation (default settings).

The receptor grid generation tool was used to create a grid representing the active site of each protein. Protein docking was carried out using the Glide Extra Precision (XP) docking module of the Virtual Screening Workflow (VSW) function in Maestro (Sánchez-Pérez et al., 2015). The default settings of VSW were used. To evaluate the docking results, the best-docked pose with the most negative Glide score value was recorded for each ligand and then compared to a cut-off docking score. The comparison between the docking score was used to distinguish the potential active and inactive compounds. The cut-off docking score is based on the average docking score of a set of known inhibitors for each protein. From the comparison, three ellagitannins and two urolithins were chosen for further evaluation in laboratory-based studies.

SiteMap was run on Maestro (Sánchez-Pérez et al., 2015) to identify alternative binding sites of the best-docked ellagitannins and urolithins on 3L4Y and 4GQR. Site maps were cropped at 4 Å from the nearest site point, and the SiteMap wizard was run using a more restrictive definition of hydrophobicity. OPLS2005 force field parameters were used for ligand and protein preparation. Receptor grids for each SiteMap binding site were generated on Maestro using the centroid coordinates of the sites as centres of search spaces. Sitemap docking simulations were performed using Glide XP.

2.3. Kinetics of ellagitannin inhibition of α-amylase

The kinetics of α-amylase in the presence and absence of ellagitannins were evaluated according to a previously described method (Adisakwattana et al., 2009). The porcine pancreatic amylase enzyme (50 μL, 0.5 U/mL) was dissolved in 20 mM phosphate buffer (pH 6.9) containing 6.7 mM NaCl, and preincubated with the ellagitannins (50 μL) for 10 min at 25 °C. The substrate, starch (100 μL, 1-10 mg/mL), was added before the reaction was stopped after 10 min by adding 100 μL DNSA (96 mM) and heating the reactions at 80 °C for 25 min. Once the reactions reached room temperature 50 μL of the contents was pipetted into a new plate and 200 μL of ddH_2O was added. The absorbance was measured at 540 nm (SpectraMax Paradigm, Molecular Devices Inc., CA, USA). The assay was repeated with three different concentrations for each inhibitor. Acarbose was used as the positive control. To account for any chemical interference, the blanks were wells containing buffer, inhibitor, starch (0–10 mg/mL) and DNSA but no enzyme. A second blank, used to account for any reducing effects on DNSA by the inhibitors, contained enzyme, inhibitor, buffer and DNSA but no starch.

2.4. Kinetics of ellagitannin inhibition of α-glucosidase

The kinetics of α-glucosidase in the presence and absence of ellagitannins were evaluated according to a previously described method (Ali et al., 2002). Briefly, in a 96-well plate (Greiner, clear, F-bottom) 50 μL of the enzyme (0.2 U/mL) diluted in 100 mM phosphate buffer (pH 6.8), was preincubated with 100 μL of the ellagitannins for 10 min at 37 °C. Thereafter, 50 μL serial concentrations of pNPG (0–1.25 mM) was added and the reaction mixtures were incubated at 37 °C for 30 min. NaOH (50 μL, 0.1M) was added to stop the reactions before the absorbance was measured at 405 nm. The assay was repeated with three different concentrations for each inhibitor. The positive control was acarbose, and blanks were wells containing no enzyme but pNPG, inhibitor, buffer and NaOH.

2.5. UPLC-MS/MS targeted analysis

25 mg of each tea sample was accurately weighed into a 2 mL centrifuge tube. At least three biological sample replicates were prepared for each tea. A volume of 1.6 mL 50% methanol/0.1% formic acid in water was added for metabolite extraction. The samples were vortexed, sonicated and centrifuged (500 xg, 5 min). The supernatants were diluted six-fold with extraction solvent and transferred into glass vials.

A cocktail of standards was prepared, containing, catechin, chlorogenic acid, corilagin, epicatechin, epicatechin gallate (ECG), epigallocatechin gallate (EGCG), gallic acid, strictinin and tellimagrandin I. Each compound was diluted in 70% acetonitrile to obtain a final concentration of 0.1 mg/mL.

The UPLC MS/MS analysis was carried out at the Central Analytical Facility at Stellenbosch University. A Waters Synapt G2 Quadrupole time-of-flight (QTOF) mass spectrometer (MS) connected to a Waters Acquity ultra-performance liquid chromatograph (UPLC) (Waters, Milford, MA, USA) was used for high-resolution UPLC-MS analysis. Analysis was performed in negative ionisation mode (ESI-), with a cone voltage of 15 V, desolvation gas at 650 L/h and desolvation temperature of 275 °C. Scanning was done from m/z 150–1500 m/z in both resolution and MSE mode. Two channels were used to obtain data in MSE mode, one at low collision energy (4 V) and a second using a collision energy ramp (40−100 V) (to obtain fragmentation data). A Waters HSS T3, 2.1 × 100 mm, 1.7 μM column was used to achieve separation. The injection volume was 2 μL and the flow rate was 0.3 mL/min with a constant column temperature of 55 °C. Solvent A was formic acid (0.1%) and solvent B was acetonitrile with 0.1% formic acid. The gradient started at 100% solvent A for 1 min and linearly changed to 28% B over 22 min. It then went to 40% B over 50 s and a wash step of 1.5 min at 100% B, followed by re-equilibration to initial conditions for 4 min.

2.6. Tea preparation

Water extracts that simulate normal tea preparation were prepared. Green and purple tea leaves were soaked in boiling water for 10 min. After brewing, the tea was poured into Falcon tubes and centrifuged for 5 min at 500 rcf, thereafter the supernatant was syringe filtered (0.2 μm). The filtered supernatant was used as a stock solution and diluted to working concentrations for enzyme assays using ddH_2O.

2.7. α-Amylase inhibition by green and purple teas

The dose-dependent α-amylase inhibitory activity of green and purple tea water extracts was performed, according to the method described by Yang and Kong (2016). In 96-well plates (Greiner, clear, F-bottom), 50 μL porcine α-amylase enzyme (0.5 U/mL) and 50 μL of serial dilutions of green or purple tea (3.75%–0.05% w/v) were preincubated for 10 min at room temperature, before 100 μL starch (2% w/v) was added. After a 10 min incubation, the reaction was stopped by adding 100 μL DNSA. The reaction mixtures were heated at 80°C for 25 min. Once the reactions reached room temperature 50 μL was pipetted into a new plate and 200 μL ddH_2O was added. The absorbance was measured at 540 nm and the percentage inhibition was calculated. The control wells contained buffer, enzyme, starch and DNSA but no inhibitor, and the blank wells contained no enzyme. Acarbose was used as the positive control.

2.8. α-Glucosidase inhibition by green and purple teas

The dose-dependent α-glucosidase inhibitory activity of green and purple tea water extracts was evaluated, according to the method described by Yang and Kong (2016). In 96-well plates (Greiner, clear, F-bottom), 25 μL α-glucosidase enzyme (0.2 U/mL) and 100 μL serial dilutions of green or purple tea (0.005% - 7.8 × 10^{-5}% w/v) were preincubated for 10 min at 37 °C. Thereafter, 50 μL pNPG (5 mM) was added and the reactions were incubated for 30 min at 37 °C. The reactions were stopped by adding 50 μL of NaOH (0.1 M). The control was wells containing buffer, enzyme, pNPG and NaOH but no inhibitor, while the blank contained no enzyme. Acarbose was used as the positive control. The absorbance was read spectrophotometrically at 405 nm and the percentage inhibition was calculated.

2.9. Cell culture

Mouse fibroblast (3T3-L1), mouse myoblast (C2C12) and human hepatoma (HepG2) cells were grown in DMEM supplemented with 10% (v/v) FCS and 1% (v/v) penicillin/streptomycin/amphotericin. All cell incubations were performed at 37°C in a humidified atmosphere of 95% air to 5% CO_2 unless otherwise stated.

2.9.1. 3T3-L1 differentiation

The differentiation of 3T3-L1 fibroblasts into adipocytes was performed according to the method described by Ibrahim et al. (2019). Briefly, 3T3-L1 fibroblasts were plated at 1 × 10^4/well and grown until confluency. Once confluent, cells were differentiated on days 4 and 7 in differentiation media (DM) 1, DMEM/FCS containing insulin (10 μg/mL), isobutyl methylxanthine (0.5 mM), dexamethasone (1 μM) and rosiglitazone (2 μM). On day 10 media was changed to DM2, DMEM/FCS containing insulin (10 μg/mL). Finally, on day 14 the cells were exposed to drugs as stipulated in each respective assay.

2.10. Sulforhodamine B (SRB) cytotoxicity assay

The cytotoxicity of the urolithins and ellagitannins was evaluated using a method previously described by Vichai and Kirtikara (2006). Cultured C2C12 and HepG2 cells were exposed to ellagitannins (100, 10, 1, 0.1, 0.01, 0.001 μM) and urolithins (100, 10, 1, 0.1, 0.01, 0.001 μM) for 72 h, while differentiated 3T3-L1 cells (differentiation method explained in section 2.9.1) were exposed for 48 h. The negative control was wells containing cells and media, the blanks were wells containing media only, and the positive control was DMSO (10%). Trichloroacetic acid (TCA) (50 μL, 50% w/v) was added to fix the cells and the plates were incubated at 4 °C for 24 h before they were washed with tap water and dried overnight. SRB dye (100 μL, 0.057% w/v) was added to each well and incubated for 30 min before the unbound dye was washed away using acetic acid (1%). Once the plates were dry, Tris buffer (200 μL, 10 mM, pH 10.5) was added to extract the bound dye. The plates were gently shaken (550 rpm) for 1 h before the absorbance was read at 540 nm (ELx800, BioTek, VT, USA). Cell viability was calculated as a percentage of the negative control.

2.11. Oil Red O (ORO) lipid accumulation assay

The ORO assay was used to evaluate the ability of the urolithins to decrease hepatic and adipocyte lipid accumulation as described by Ibrahim et al. (2019) and Tshiyoyo et al. (2022) respectively. 3T3-L1 and HepG2 cells were seeded in 96-well plates at a density of 1 × 10^4 and 5 × 10^4 cells/well, respectively and were left overnight to allow attachment. The fibroblasts were differentiated into adipocytes (differentiation method explained in section 2.9.1), and HepG2 cells were treated with 1 mM oleic acid for 48 h to stimulate lipid accumulation. The cells were treated with non-cytotoxic concentrations (0.01, 0.1, 1 and 10 μM) of urolithin A or urolithin B for 48 h. The control wells were cells treated with oleic acid only for the HepG2 experiment and cells only (no treatment) for the 3T3-L1 experiment. The positive control was metformin (65 μM), and the blank was isopropanol only. After treatment, the cells were fixed with 2% (v/v) formalin for 30 min at 37 °C. For staining, a fresh ORO working solution, diluted 1.7x in ddH2O and filtered (Munkiel 185 mm filter paper) was prepared from a stock ORO solution (5% in 60% isopropanol) before use. The fixing solution was discarded before staining with 100 μL of the ORO working solution for 1 h. The stain was then removed, and the plates were washed with tap water and dried. Images were captured with a microscope (TH4-200, Olympus Corporation, TYO, JPN). For quantification, the ORO dye was extracted with 100 μL 60% (w/v) isopropanol and the absorbance was measured at 405 nm (FLUOstar Omega, BMG Labtech, BW, DEU). The results are expressed as the percentage of lipid accumulation relative to the control.

2.12. 2-NBDG glucose uptake assay

The effect of urolithins on glucose uptake was evaluated on C2C12, HepG2 and differentiated 3T3-L1 cells, using the fluorescent probe 2-NBDG. The experiment was carried out according to the method by Dayarathne et al. (2021), with modifications. Once confluent and attached, the DMEM medium of cultured C2C12, HepG2 and differentiated 3T3-L1 cells (differentiation method explained in section 2.9.1) was aspirated and replaced with 100 μL glucose-free DMEM (supplemented with 2.5% FCS). After 24 h the glucose-free media was aspirated, and the cells were treated with non-cytotoxic concentrations (0.01, 0.1, 1 and 10 μM) of urolithin A and urolithin B. The control wells contained cells, dye, and no treatment. Metformin (65 μM) was used as a positive control, and the blank was wells containing PBS only. After 24 h of incubation, the media was aspirated and the cells were incubated with 100 μL 2-NBDG dye (100 μM) for 1 h, in the dark. The dye was removed, and PBS (100 μL) was added. The fluorescent intensities of the cells were quantified using a fluorometer (Synergy 2, BioTek, VT, USA) at λ_{ex} = 485 nm and λ_{em} = 590 nm and the relative fluorescent units were calculated.

2.13. Data analysis

All experiments were carried out in triplicate and at least three independent experiments were performed. TargetLynx XS (Waters) was

used to integrate peak areas to obtain relative concentrations of the ellagitannins (and other standards) in the purple and green tea samples. The results are expressed as the mean ± standard error of the mean (SEM). The statistical significance was calculated using a one-sided Student's t-test, by considering the concentration of the specified metabolite across the green tea and the purple tea samples. GraphPad Prism (version 8.0.2) was used to analyse the data, and to calculate the IC_{50} values. Data were analysed using Student's t-tests, and differences were considered significant at $p < 0.05$.

3. Results and discussion

3.1. In silico docking

Fifty tea ellagitannins and urolithins were identified through the literature review and were docked to nine antidiabetic protein targets (identified from DIA-DB) using Maestro (Schrodinger LLC, 2021). These were two glucose-regulating targets, α-glucosidase (3L4Y) and α-amylase (4GQR), six insulin secretion and/or sensitivity-regulating targets, retinol-binding protein (2WR6), insulin receptor precursor (3EKN), tyrosine-protein phosphatase (4GE6), corticosteroid dehydrogenase (4K1L), dipeptidyl peptidase (4A5S) and fatty acid receptor 1 (4PHU), and one lipid metabolism-regulating target, peroxisome proliferator-activated gamma (2FVJ) (Table 1).

Corilagin, strictinin, tellimagrandin I, urolithin A and urolithin B (Fig. 1) were identified as the ellagitannins and urolithins with the best docking scores across the targets (Table 1). Overall, the docking scores of the ellagitannins were more negative than those of drugs currently on the market (cut-off docking score in Table 1). The ellagitannins were expected to have good docking scores, as these are large molecules with many hydroxyl groups that can form favourable hydrogen bonds with the protein and the large size of the molecules fit well within the binding pockets of the proteins. The results in Table 1 show that the ellagitannins (corilagin, strictinin, tellimagrandin I) have better (more negative) docking scores than the cut-off value when docked to 3L4Y and 4GQR. All the compounds (ellagitannins and urolithins) have better docking scores than the cut-off value when docked to 3EKN and 4A5S. Maestro did not generate docking scores for the ellagitannins when docked to 2WR6 probably due to the ellagitannins being too large to fit within the binding pocket of 2WR6, however the urolithins have better docking scores than the cut-off value for 2WR6. All the compounds besides tellimagrandin I have better docking scores than the cut-off value for 4K1L. Strictinin and tellimagrandin I have better docking scores than the cut-off value for 4GE6. None of the compounds had better docking scores than the cut-off value when docked to 2FVJ and 4PHU.

3.2. Kinetics of ellagitannin inhibition of α-amylase and α-glucosidase

Alpha-amylase and α-glucosidase are enzymes in the GIT mucosa involved in starch digestion. Starch is hydrolysed by α-amylase to produce maltose, maltotriose and dextrins, which are further digested by α-glucosidase in the small intestine. The main product of α-glucosidase digestion is glucose, which is actively transported into the bloodstream, increasing plasma glucose (Proença et al., 2017). Therefore, an effective approach to manage postprandial hyperglycaemia is to partially inhibit α-amylase and α-glucosidase activity, thus delaying the postprandial surge of glucose.

Based on the high negative docking scores (Table 1) of the ellagitannins to α-glucosidase (3L4Y) and α-amylase (4GQR) their inhibitory activity was evaluated *in vitro*, compared to acarbose the current gold standard α-amylase and α-glucosidase inhibitor. Acarbose was identified and verified as a mixed inhibitor of α-amylase (Proença et al., 2019) and a competitive inhibitor of α-glucosidase (Proença et al., 2017). Corilagin, strictinin and tellimagrandin I inhibited α-amylase and α-glucosidase in a dose-dependent manner. As shown in Fig. S6 and Table 2, strictinin was a competitive inhibitor of α-glucosidase, while corilagin was a non-competitive inhibitor. Tellimagrandin I uncompetitively inhibited α-glucosidase. As shown in Fig. S7 and Table 2, strictinin and tellimagrandin I inhibited α-amylase competitively, while corilagin was a mixed inhibitor of α-amylase.

Competitive inhibitors compete with substrates for binding to the orthosteric binding site (OBS) of enzymes, whereas uncompetitive and non-competitive inhibitors bind to allosteric binding sites (ABS) apart from OBS (Mazzei et al., 2016). To predict the possible *in silico* binding site(s) of the uncompetitive and non-competitive inhibitors, SiteMap (Schrodinger LLC, 2021) was run. The docking studies included the highest-scoring five sites detected by SiteMap (Table 3). SiteMap evaluates sites in terms of steric and electrostatic properties and scores each site using these terms. Strictinin and acarbose were identified as *in vitro* competitive inhibitors of α-glucosidase. The *in silico* Sitemap docking results (Table 3) confirmed that these compounds had the best docking score to the orthosteric substrate binding site of 3L4Y, corresponding to competitive inhibition observed in the *in vitro* enzyme studies. The uncompetitive α-glucosidase inhibitor, tellimagrandin I, showed strong binding to ABS2. Unlike the uncompetitive inhibitor, corilagin is a non-competitive inhibitor of α-glucosidase (3L4Y), and thus likely bound to a different allosteric site, namely ABS1. Strictinin and tellimagrandin I had the best docking score to the OBS of α-amylase (4GQR), corresponding to the competitive inhibition in the *in vitro* enzyme studies. Corilagin and acarbose are mixed-competitive inhibitors of α-amylase (4GQR), thus strong binding to the OBS and an ABS is expected. Acarbose had very similar docking scores to OBS and ABS2

Table 1
Glide XP docking scores (Kcal/mol) of best-docked ellagitannins and urolithins to protein targets (PDB code) regulating glucose metabolism, insulin sensitivity and secretion, and lipid metabolism.

		Glucose metabolism regulating protein targets		Insulin secretion and sensitivity regulating protein targets						Lipid metabolism regulating protein target
		3L4Y	4GQR	2WR6	3EKN	4GE6	4K1L	4A5S	4PHU	2FVJ
Test compounds	Corilagin	**−10.7**	**−12.0**	n/a	**−8.6**	−9.1	**−13.8**	**−8.8**	n/a	n/a
	Strictinin	**−13.2**	**−11.9**	n/a	**−8.3**	**−10.7**	**−12.9**	**−8.6**	−5.1	n/a
	Tellimagrandin I	**−13.1**	**−14.1**	n/a	**−8.8**	**−12.9**	n/a	**−9.9**	n/a	−3.7
	Urolithin A	−4.9	−5.6	**−8.9**	**−7.6**	−2.9	**−7.6**	**−8.4**	−5.3	−6.7
	Urolithin B	−4.5	−5.1	**−8.9**	**−8.1**	−2.2	**−6.7**	**−8.0**	−7.8	−7.2
	Positive control cut-off value	−9.2	−8.6	−6.5	−7.5	−9.4	−6.3	−6.7	−13.1	−9.7

Cut-off value defined as the sum of the average docking score of gold-standard drugs.
n/a = no docking score generated.
Bold text = docking score better (more negative) than cut-off docking score.
α-glucosidase (3L4Y), α-amylase (4GQR), retinol-binding protein (2WR6), insulin receptor precursor (3EKN), tyrosine-protein phosphatase (4GE6), corticosteroid dehydrogenase (4K1L), dipeptidyl peptidase (4A5S) and fatty acid receptor 1 (4PHU), peroxisome proliferator-activated gamma (2FVJ).

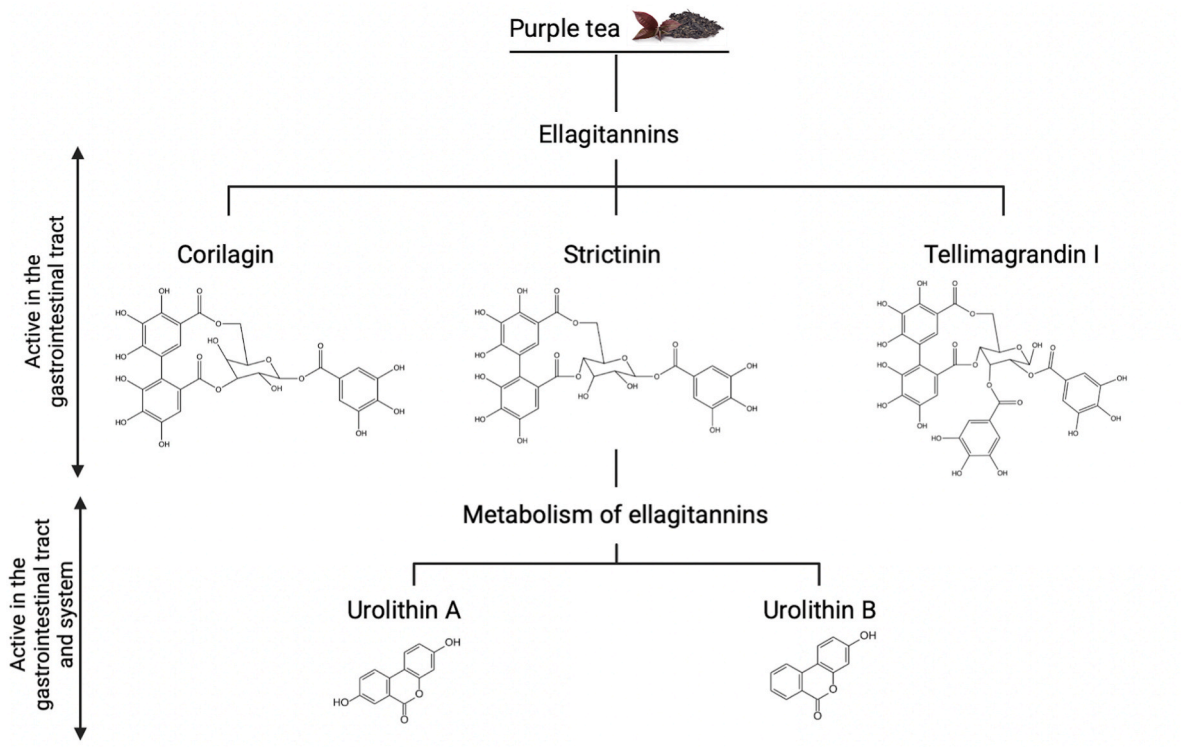

Fig. 1. Structure and sites of activity of the best-docked ellagitannins and their metabolites, urolithins (Structures were drawn with ChemDraw v19.1).

Table 2
Inhibitory activity of ellagitannins against α-glucosidase and α-amylase.

Compound	K_i (μM) (α-glucosidase)	Type of inhibition (α-glucosidase)	K_i (μM) (α-amylase)	Type of inhibition (α-amylase)
Strictinin	0.11 ± 0.03*	Competitive	1.55 ± 0.36*	Competitive
Tellimagrandin I	0.12 ± 0.01*	Uncompetitive	0.20 ± 0.03*	Competitive
Corilagin	0.33 ± 0.13*	Non-competitive	0.55 ± 0.08*	Mixed-competitive
Acarbose (positive control)	472 ± 35	Competitive	2.31 ± 0.22	Mixed-competitive

Data are represented as mean ± SEM (n = 3).
*K_i values significantly lower ($p < 0.05$) than acarbose (determined using a one-sided Student's t-test).

Table 3
Glide XP docking scores (Kcal/mol) of the ellagitannins to the orthosteric binding site (OBS) and allosteric binding sites (ABS) of 3L4Y and 4GQR.

	OBS		ABS1		ABS2		ABS3		ABS4		ABS5	
	4GQR	3L4Y	4GQR	3L4Y	4GQR	3L4Y	4GQR	3L4Y	4GQR	3L4Y	4GQR	3L4Y
Acarbose	−9.9	**−8.2**	n/a	−7.4	**−10.7**	−6.1	−9.3	−7.1	n/a	−7.8	−7.6	−7.3
Corilagin	**−12.0**	−10.7	n/a	**−11.7**	−9.1	−9.2	−9.8	−8.8	−5.1	−9.2	−6.9	−7.0
Strictinin	**−11.9**	**−13.2**	n/a	−10.3	−9.6	−9.6	−9.7	−9.1	−2.3	−9.7	n/a	−7.3
Tellimagrandin I	**−14.1**	−13.1	n/a	−12.6	−11.9	**−13.7**	−10.3	−12.1	n/a	−10.3	n/a	−5.4

n/a = no docking score generated.
Bold text = Binding site with the best docking score (for each ellagitannin).
α-glucosidase (3L4Y), α-amylase (4GQ.

of α-amylase (4GQR), which explains the mixed-competitive inhibition observed with the *in vitro* enzyme studies. Corilagin docked the best within the OBS and ABS3 of α-amylase (4GQR).

K_i values reflect the functional strength of an inhibitor and are useful to compare the inhibitory activity of compounds. High binding affinity between an inhibitor and enzyme is indicated by a low K_i value. Acarbose's K_i values (Table 2) for α-amylase (Proença et al., 2019) and α-glucosidase (Proença et al., 2017) correspond well with literature. The ellagitannins had significantly lower ($p < 0.05$) K_i values than acarbose when inhibiting α-amylase and α-glucosidase. For α-glucosidase, the K_i values (Table 2) of the ellagitannins were approximately 4000 times smaller than acarbose, indicating potent inhibition of the enzymes by the ellagitannins. For α-amylase, the K_i values (Table 2) for the ellagitannins were approximately 30 times smaller than the K_i value of acarbose. The binding affinity of the ellagitannins to α-amylase was weaker than to α-glucosidase, however this result is not necessarily undesirable since the inhibition of α-amylase has been associated with abdominal discomfort due to polysaccharide fermentation (Proença et al., 2019). This implies that a weak α-amylase inhibitor in the presence of a strong α-glucosidase inhibitor may be preferred.

The relationship (Fig. S8) between the *in vitro* inhibitory strength and *in silico* docking results was determined. The correlation between the K_i

values and docking scores of the ellagitannins, to α-amylase and α-glucosidase, are shown in Fig. S8. A positive relationship between the docking scores of the ellagitannins and the K_i values of ellagitannins is suggested by the positive slope of the graphs. A high negative docking score corresponds to a low K_i value, both indicating more potent inhibition.

3.3. Targeted UPLC-MS/MS analysis

Due to the potent *in vitro* inhibition of α-amylase and α-glucosidase by the ellagitannins, it was determined whether these ellagitannins are present in commercial green and purple teas. The ellagitannins, corilagin, strictinin and tellimagrandin I were quantified in six commercial purple and six commercial green teas, using UPLC-MS/MS. Along with the ellagitannins, six other common tea metabolites, catechin, chlorogenic acid, epicatechin, ECG, EGCG and gallic acid were also identified and quantified using authentic standards (Table 4). The retention times as well as the UPLC chemical profile of the compounds are listed in Table S1 (supplementary info).

The ellagitannins were identified and quantified in purple and green teas, and it was determined that the abundance of corilagin, strictinin and tellimagrandin I were significantly higher ($p < 0.05$) in purple tea samples compared to green tea samples. Strictinin and tellimagrandin I were only detected in trace amounts (Table 4), however high concentrations of corilagin were present in the green-purple teas. Corilagin were on average present at double the concentration of catechin and half the concentration of EGCG – two major tea metabolites. Furthermore, the purple teas had a significantly higher ($p < 0.05$) abundance of chlorogenic acid, ECG and gallic acid than the green teas. The higher concentration of flavonoids in purple teas contributes to the health benefits of these teas.

3.4. α-Amylase and α-glucosidase inhibition by green and purple teas

Camellia sinensis teas are widely available, easy to store and affordable, and due to the ellagitannin (especially corilagin) content in purple teas their α-amylase and α-glucosidase inhibitory activity were determined. The IC_{50} values (Table 5) of commercial green and purple teas against α-amylase and α-glucosidase were calculated from dose-response curves (Figs. S2–S5) and compared to acarbose. The IC_{50} values (Table 5) of acarbose for α-amylase and α-glucosidase were similar to those reported by Alqahtani et al. (2019) and Hossain et al. (2020) respectively. All teas inhibited α-glucosidase more effectively than acarbose, with the IC_{50} of Sun Rouge, being 400 times lower than

Table 5
IC_{50} values of green and purple teas, and acarbose against α-amylase and α-glucosidase.

	Tea type	IC_{50} (μg/mL) α-Glucosidase	IC_{50} (mg/mL) α-Amylase
Sun Rouge	Purple (Green-Purple)	$2.14 \pm 0.14^{*,+}$	$5.36 \pm 1.03^{\#}$
Finlays	Purple (Green-Purple)	$4.35 \pm 0.18^{*}$	$7.77 \pm 0.45^{\#}$
Tumoi Nandi Hills	Purple (Green-Purple)	$4.47 \pm 0.38^{*}$	$6.20 \pm 2.18^{\#}$
Twinings	Green	$4.55 \pm 1.05^{*}$	24.14 ± 6.21
Zi Ya	Purple (Pu-erh – Purple)	$5.15 \pm 0.93^{*}$	36.42 ± 12.34
Dilmah	Green	$6.96 \pm 0.67^{*}$	14.60 ± 5.31
Eves	Green	$7.05 \pm 0.76^{*}$	24.23 ± 9.09
Tetley	Green	$9.29 \pm 0.45^{*}$	21.11 ± 6.69
Five Roses	Green	$11.61 \pm 3.89^{*}$	30.12 ± 4.71
Livewell	Green	$12.02 \pm 0.87^{*}$	23.45 ± 12.83
Dian Hong Jing Mai	Purple (Black -Purple)	$14.04 \pm 2.29^{*}$	17.56 ± 0.43
Dian Hong Feng Qing	Purple (Black -Purple)	$15.97 \pm 1.05^{*}$	24.72 ± 1.61
Dian Hong Sheng	Purple (Black -Purple)	$17.85 \pm 2.71^{*}$	16.37 ± 2.53
Acarbose		**807 ± 120**	**0.004 ± 0.0005**

Data are represented as mean ± SEM (n = 3).
*IC_{50} values, for α-glucosidase, significantly lower ($p < 0.05$) than acarbose (determined with a one-sided Student's t-test).
$^{+}IC_{50}$ values, for α-glucosidase, significantly lower ($p < 0.05$) than the green tea with the lowest IC_{50} (Twinings), (determined with a one-sided Student's t-test).
$^{\#}IC_{50}$ values, for α-amylase, significantly lower ($p < 0.05$) than the green tea with the lowest IC_{50} (Dilmah), (determined with a one-sided Student's t-test).

Table 4
Abundance (μg/g dry weight of tea) of ellagitannins and polyphenols in commercial green and purple teas.

	Compound	Catechin	Chlorogenic acid[a]	Corilagin[a]	EGCG	Epicatechin	ECG[a]	Gallic acid[a]	Strictinin[a]	Tellimagrandin I[a]
Green teas	Dilmah	926 ± 105	203 ± 36	590 ± 149	2237 ± 488	1602 ± 250	1941 ± 94	446 ± 28	0.2 ± 0.1	5.9 ± 0.7
	Eves	539 ± 39	365 ± 18	754 ± 121	1496 ± 333	857 ± 69	1530 ± 184	411 ± 62	n/a	2.7 ± 0.3
	Livewell	768 ± 202	38 ± 6	310 ± 86	1654 ± 17	841 ± 131	1314 ± 212	356 ± 35	0.03 ± 0.01	0.4 ± 0.1
	Five Roses	415 ± 69	152 ± 18	716 ± 103	2110 ± 376	799 ± 166	1399 ± 288	340 ± 66	n/a	1.6 ± 0.7
	Tetley	421 ± 113	295 ± 104	611 ± 141	2478 ± 648	836 ± 297	1434 ± 247	405 ± 51	1.3 ± 0.2	1.8 ± 0.8
	Twinings	561 ± 78	45 ± 12	458 ± 156	1989 ± 833	843 ± 288	1462 ± 388	423 ± 113	0.3 ± 0.1	1.6 ± 0.
Purple teas	Dian Hong Jing	714 ± 33	16 ± 11	823 ± 25	1052 ± 92	660 ± 96	1622 ± 88	1638 ± 375	0.2 ± 0.1	2.2 ± 0.4
	Dian Hong De Hong	227 ± 55	29 ± 9	352 ± 44	574 ± 73	246 ± 68	751 ± 101	902 ± 101	0.4 ± 0.1	15.4 ± 1.7
	Dian Hong Feng	146 ± 52	946 ± 283	769 ± 110	676 ± 86	285 ± 89	2488 ± 514	1658 ± 438	2.2 ± 0.6	1.1 ± 0.4
	Zi Ya	28 ± 2	99 ± 1	1754 ± 468	139 ± 42	75 ± 24	393 ± 47	585 ± 55	2.2 ± 0.5	2.1 ± 0.4
	Sun Rouge	1314 ± 389	686 ± 16	3492 ± 1024	6995 ± 1556	1072 ± 235	3403 ± 624	362 ± 126	6.4 ± 0.8	5.2 ± 0.9
	Finlays	1198 ± 261	3533 ± 610	3884 ± 740	5779 ± 1095	2273 ± 408	5846 ± 1116	1541 ± 362	2.1 ± 0.5	29.4 ± 5.3
	Tumoi Nandi Hills	675 ± 136	1806 ± 197	1914 ± 201	4077 ± 212	2439 ± 352	3786 ± 694	688 ± 143	3.5 ± 0.6	3.2 ± 0.3

Data are represented as mean ± SEM (n = 3).
n/a = not detected.
[a]compounds with a significantly higher ($p < 0.05$) abundance in purple teas than in green teas (calculated with a one-sided Student's t-test).

acarbose. The teas did not inhibit α-amylase as effectively as acarbose. Nonetheless, Sun Rouge was identified as the tea with the most effective inhibition of α-amylase. However, as mentioned earlier weaker inhibition of α-amylase is preferred (Proença et al., 2019).

The purple teas used in this study were further grouped according to their oxidation level. Sun Rouge, Tumoi Nandi Hills and Finlays were classified as green-purple variants, while the three Dian Hong teas were classified as black-purple variants and the Zi Ya tea was a pu-erh purple tea variant. The results showed that the green-purple teas had much lower IC_{50} values (Tables 5, S2 and S3), for both α-amylase and α-glucosidase than the other commercial green and purple teas, indicating that the green-purple teas had higher inhibition potency.

Urolithins are the microbial degradation products of ellagitannins (Espin et al., 2007; Villalba et al., 2019). Ellagitannins were shown to be present in purple teas (Table 4), therefore drinking purple tea would lead to the formation of urolithins in the GIT (Yang and Tomas-Barberan, 2019). The ellagitannins, corilagin, strictinin and tellimagrandin I, present in purple teas are not bioavailable, however their metabolites urolithin A and urolithin B are bioavailable. Since bioavailability is an important consideration when assessing systemic effects further experimentation focused on the bioavaialable urolithins (Fig. 1).

3.5. Cytotoxicity

Multifunctional compounds must be non-toxic to mammalian cells for therapeutic purposes, and the cytotoxicity of the compounds had to be evaluated before subsequent cell assays were performed. The SRB assay was used to assess the cytotoxicity of ellagitannins and urolithins against the differentiated 3T3-L1 adipocytes and C2C12 and HepG2 cell lines. Metformin, a bioavailable antidiabetic drug, and acarbose were included as reference compounds while DMSO was included as a positive control. DMSO caused significant ($p < 0.05$) loss of 3T3-L1 adipocyte (Fig. 2A and S9), C2C12 (Fig. 2B and S10), and HepG2 (Fig. 2C and S11) cell viability, greater than the test compounds. The ellagitannins and urolithin B did not cause a major loss of adipocyte, C2C12 and HepG2 viability (Fig. 2) and were not more cytotoxic than metformin ($p > 0.05$). Urolithin A caused a decrease in cell viability in a dose-dependent manner in hepatocytes (Fig. 2C and S11), with a 60% loss in cell viability at 100 μM, the highest concentration tested. Qui et al. (2018), reported similar results, where urolithin A but not urolithin B had a cytotoxic effect (more than a 50% decrease in cell viability) in hepatocytes.

According to Wang et al. (2015), urolithin A causes cytotoxicity in hepatocytes via suppression of β-catenin signalling, upregulation of tumour protein p53, p38 mitogen-activated protein kinases, and caspase-3 expression. In addition, the levels of intracellular reactive oxygen species are reduced and the activity of intracellular superoxide dismutase and glutathione peroxidases is increased.

3.6. Glucose uptake

Differentiated 3T3-L1 adipocytes, and C2C12 and HepG2 cells were exposed to a urolithin concentration range (0.01, 0.1, 1 and 10 M) that did not adversely affect cell viability. The effect on glucose uptake was determined with the 2-NBDG assay. Metformin, an antidiabetic drug, that increases cellular glucose uptake was used as a positive control (Polianskyte-Prause et al., 2019). The cells were treated with a range of non-cytotoxic urolithin A and urolithin B concentrations (0.01, 0.1, 1 and 10 μM), to determine whether the urolithins had an effect on cellular glucose uptake. Metformin (65 μM) and the two highest tested concentrations (1 and 10 μM) of the urolithins, significantly increased ($p < 0.05$) glucose uptake in all the tested cell lines, in comparison with the no treatment control (Fig. 3). Urolithin A (10 μM) and urolithin B (10 μM) caused a significantly ($p < 0.05$) higher increase in glucose uptake in all the cell lines, compared to metformin (65 μM) (Fig. 3).

At 10 μM in all cell lines, urolithin A and urolithin B, caused a significant increase in glucose uptake when compared with 65 μM metformin. Based on the docking results, the urolithins have especially good docking scores to three insulin secretion and sensitivity-regulating targets, these are retinol-binding protein (2WR6), insulin receptor precursor protein (3EKN) and corticosteroid dehydrogenase (4K1L). Therefore it can be hypothesised that strong binding to these targets led to increased glucose uptake in adipocytes, C2C12 cells and HepG2 cells, however gene expression studies will provide a better understanding of the mechanism of action.

3.7. Lipid accumulation

Fatty liver disease and perivascular lipid accumulation are both common comorbidities of T2DM (Ibrahim et al., 2019). Therefore, the prevention or treatment of lipid accumulation has an important role in the management of T2DM. The effects of urolithin A and urolithin B were compared to metformin, an antidiabetic drug that in addition to controlling glucose uptake also reduces lipid accumulation (Chen et al., 2018) in adipocytes and hepatocytes was determined, using the ORO assay. The extracted ORO is proportional to the amount of lipid formed and is thus a quantitative measure of lipid accumulation (Mehlem et al., 2013).

In the 3T3-L1 differentiated adipocytes and the HepG2 cells, lipid accumulation occurred, and ORO showed red cellular staining (Fig. 4A and C) where exposure to urolithin A and urolithin B, caused a reduction in the extent or intensity of staining. The accumulation of lipids was then quantified following ORO extraction (Fig. 4B and D). For urolithin A and urolithin B, there was a significant decrease in lipid accumulation compared to the control ($p < 0.05$). Compared with 65 μM metformin, urolithin A (10 μM) and urolithin B (10 μM) were significantly ($p < 0.05$) more effective in reducing lipid accumulation.

When higher amounts of glucose are taken up by adipose cells, it is converted into triglycerides and increased lipid accumulation is expected (Perera et al., 2020). Here urolithins could enhance glucose uptake and decrease lipid accumulation, ellagitannins evaluated by Perera et al. (2020) and Kowalska et al. (2014) displayed a similar effect in adipocytes. Expression studies examining several genes such as C/EBPα and PPARγ will provide a better understanding of the mechanistic pathway of urolithin A and urolithin B (Kowalska et al., 2014).

In this study, it is shown that urolithins enhance glucose uptake having a beneficial effect on hepatic and adipose tissue which in T2DM is non-responsive to insulin. In addition, the reduction in lipid accumulation, often associated with T2DM, is a further beneficial effect. Both Perera et al. (2020) and Kowalska et al. (2014) showed that ellagitannins had a similar effect. Furthermore, the anti-inflammatory effect of urolithins is well described (Villalba et al., 2019; Zhang et al., 2021), especially related to its beneficial effect on pancreatic inflammation which plays a key role in diabetes pathogenesis and progression (Zhang et al., 2021) which thus identifies the urolithin A and urolithin B as multifunctional molecules, that effectively target several aspects of T2DM.

4. Conclusion

In conclusion, docking studies indicated that strictinin, corilagin and tellimagrandin I have strong binding to antidiabetic targets, including α-glucosidase and α-amylase. In vitro enzyme assays revealed that the ellagitannins are potent dual inhibitors of α-glucosidase and α-amylase. A good correlation was found between *in silico* enzyme inhibition evaluated using docking analysis and *in vitro* inhibition efficacy using enzymatic assays. Commercial purple teas were identified as a source of ellagitannins, with higher ($p < 0.05$) concentrations of corilagin, strictinin and tellimagrandin I than green teas. Green-purple teas were identified as potent α-glucosidase inhibitors, with IC_{50} values lower than green teas. Urolithin A and urolithin B enhanced glucose uptake in

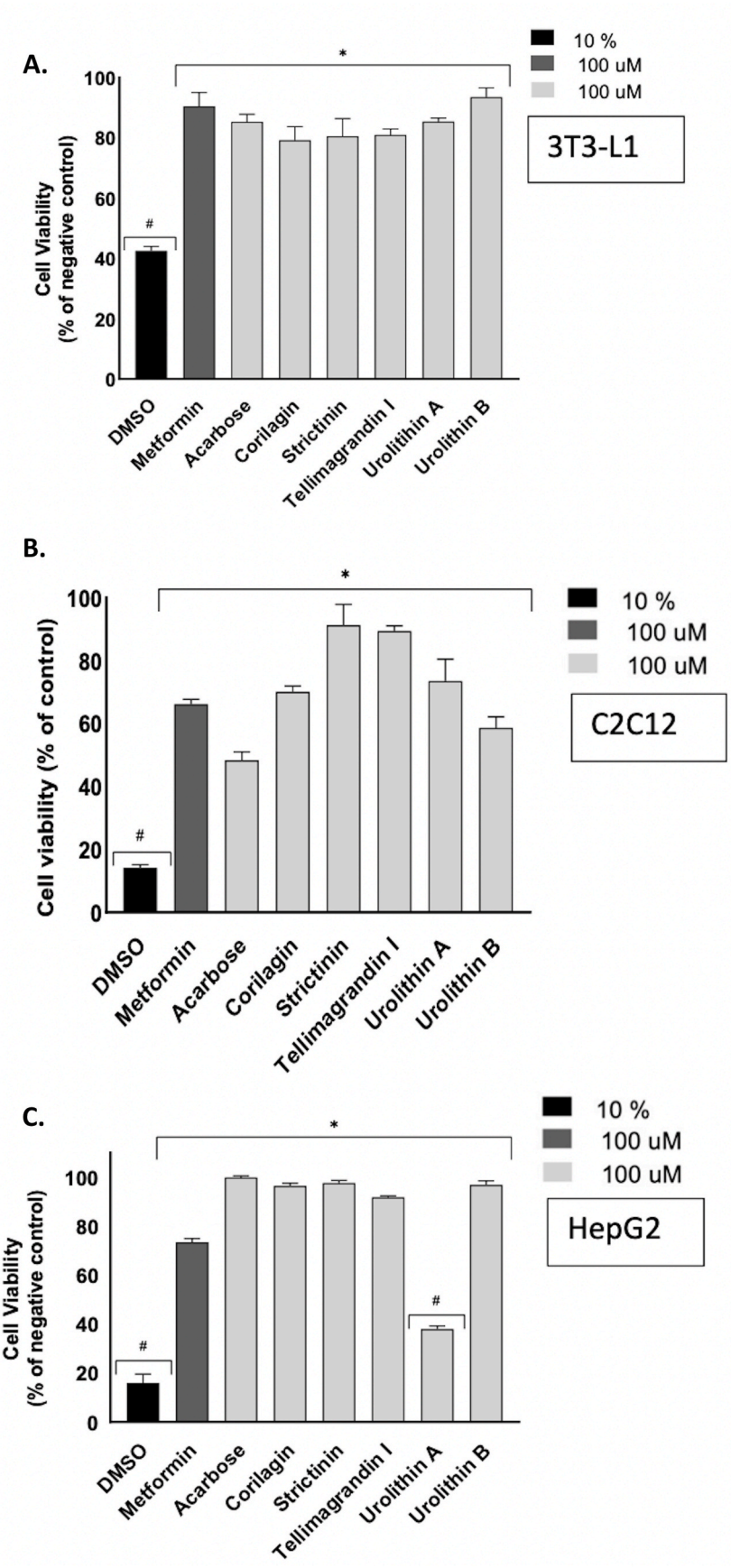

Fig. 2. The effect of the highest tested concentration (100 μM) urolithins and ellagitannins on cell viability (n = 3, SEM error bars) **(A.)** 3T3-L1 adipocytes, **(B.)** C2C12 cells, and **(C.)** HepG2 cells. Cell viability (in the presence of the compounds) was expressed as a percentage of the negative control (cells with no drug added). *Cell viability significantly different ($p < 0.05$) from positive control (DMSO) (calculated using a two-sided Student's t-test). #Cell viability significantly lower ($p < 0.05$) than metformin (calculated using a one-sided Student's t-test).

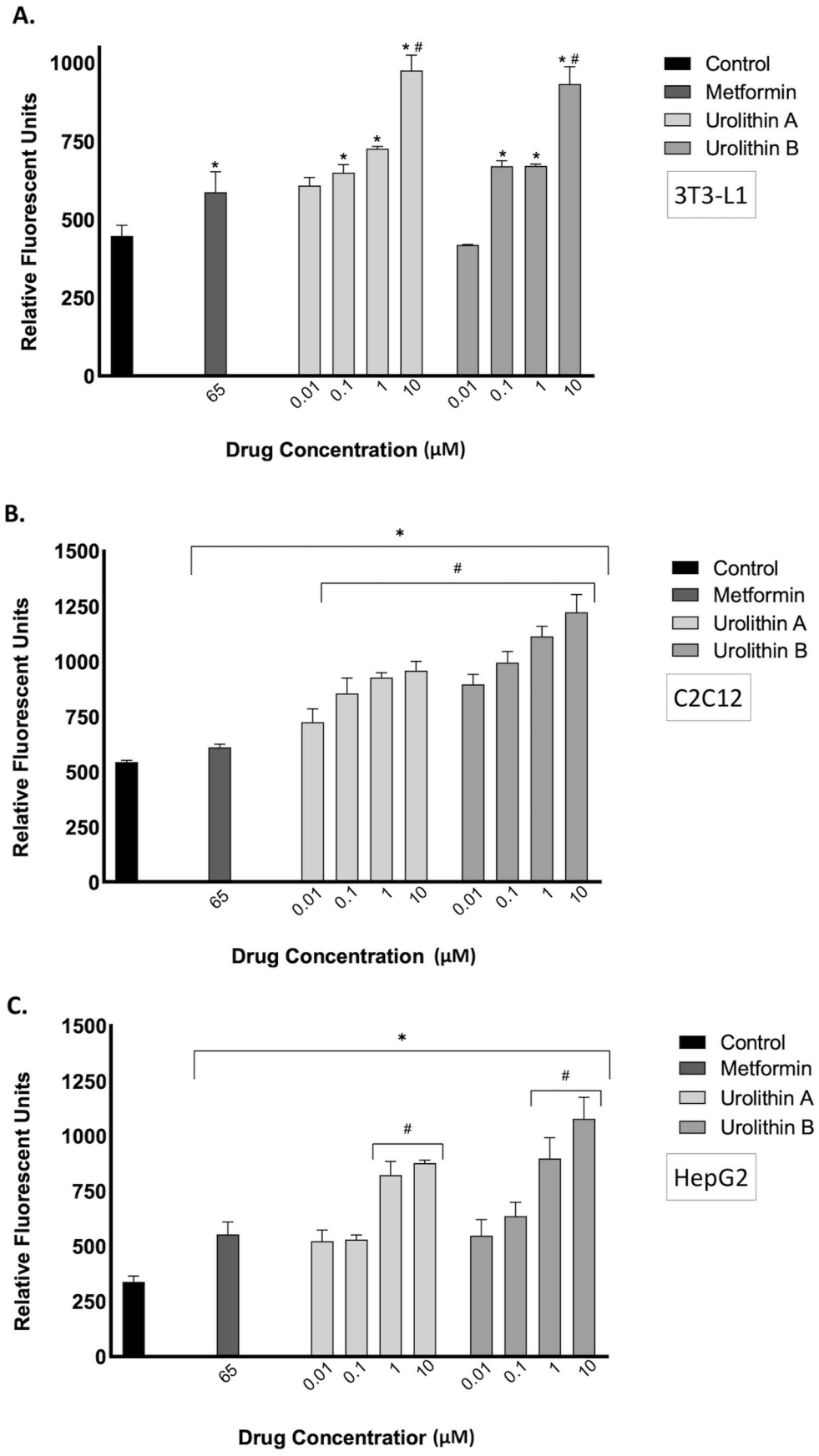

Fig. 3. Effect of urolithins on glucose uptake on **(A.)** 3T3-L1 differentiated adipocytes, **(B.)** C2C12 cells and **(C.)** HepG2 hepatocytes. Cells were exposed to urolithins for 48 h. Data are represented as mean ± SEM. *Glucose uptake significantly different ($p < 0.05$) from control (cells with no drugs added) (calculated using a two-sided Student's t-test). #Glucose uptake significantly higher ($p < 0.05$) than metformin (calculated using a one-sided Student's t-test).

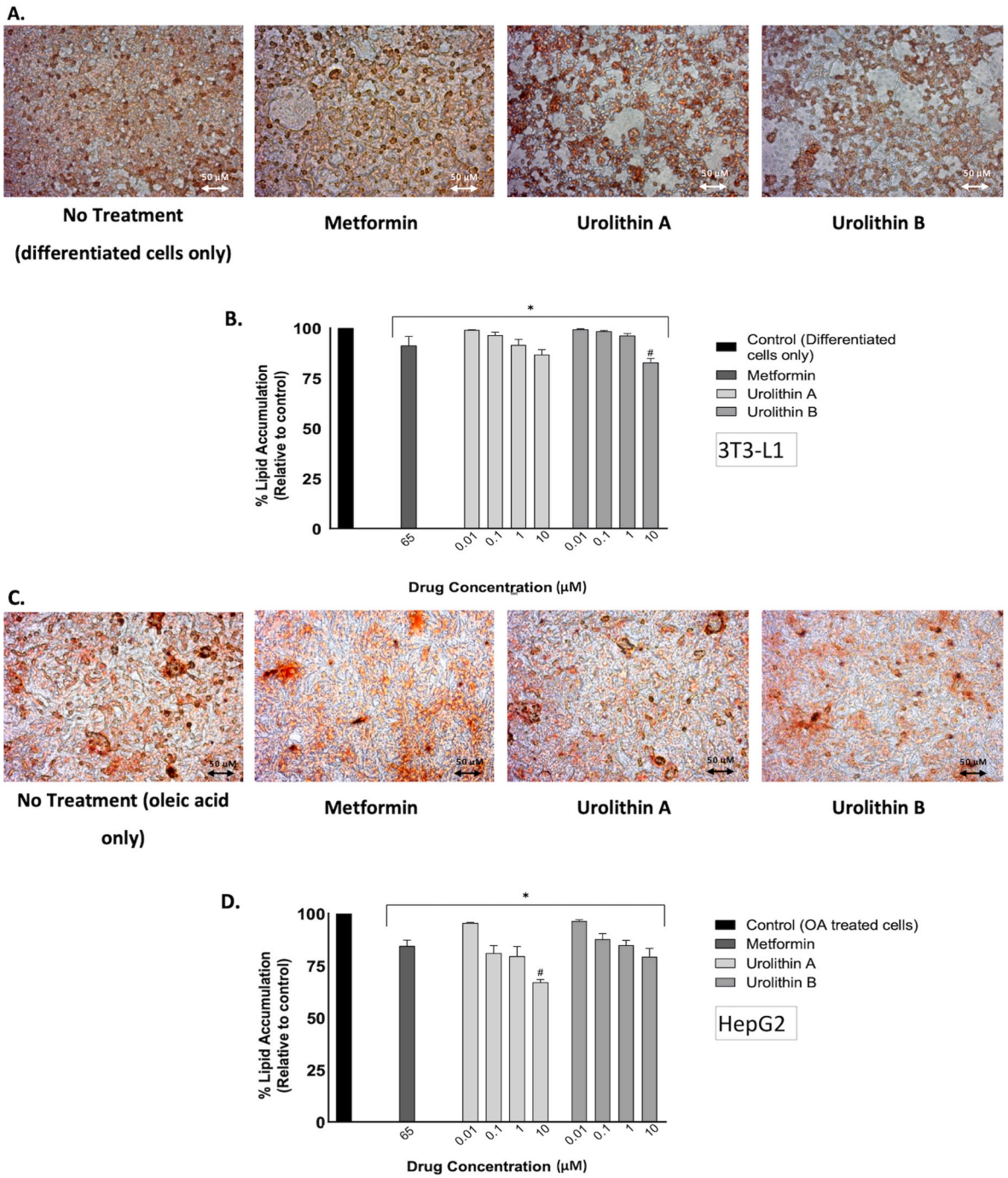

Fig. 4. Micrographs showing the lipid accumulation in cells **(A.)** 3T3-L1 differentiated adipocytes and **(C.)** HepG2 hepatocytes in the presence of urolithin A (10 μM), urolithin B (10 μM) and metformin (65 μM) (control). The cells were photographed at magnification X20 and the scale bar represents 50 μM. Quantitative analysis of urolithins on lipid accumulation in Oil red O-stained **(B.)** 3T3-L1 differentiated adipocytes and **(D.)** HepG2 hepatocytes. Cells were exposed to urolithins for 48 h. Lipid accumulation was calculated as a percentage relative to the control. Data are represented as mean ± SEM. *Lipid accumulation significantly different ($p < 0.05$) from the control (calculated using a two-sided Student's t-test). #Lipid accumulation significantly lower ($p < 0.05$) than metformin (calculated using a one-sided Student's t-test). (For interpretation of the references to colour in this figure legend, the reader is referred to the Web version of this article.)

adipocytes, C2C12 cells and HepG2 cells, and decreased lipid accumulation in adipocytes and HepG2 cells. The ability of urolithins to stimulate glucose uptake without causing lipid accumulation in cells would be advantageous, as an anti-hyperglycaemic drug for T2DM, as it may be able to control blood sugar levels without causing weight gain as a side effect.

Thus, drinking green-purple teas can potentially inhibit α-amylase and α-glucosidase, and the ellagitannins present in the teas will be metabolised to urolithins. Urolithins can in turn enhance glucose uptake in adipose, muscle cells and hepatocytes, while also decreasing lipid accumulation in adipocytes and hepatocytes. Consequently, these multifunctional compounds target starch degradation, glucose uptake, and hepatic and perivascular lipid accumulation with minimal toxic effects, however these statements need to be confirmed *in vivo,* by testing purple teas on a diabetic rat model.

This manuscript may encourage others to search for cultivars of green-purple teas that have higher concentrations of ellagitannins, such as corilagin. These results may also encourage others to investigate tea

factory processing and field agronomic practices that may increase the content of ellagitannins in teas.

CRediT authorship contribution statement

M. Tolmie: Conceptualization, Investigation, Resources, Formal analysis, Writing – original draft, Writing – review & editing, Visualization. **M.J. Bester:** Conceptualization, Writing – review & editing, Supervision. **J.C. Serem:** Conceptualization, Investigation, Writing – review & editing. **M. Nell:** Investigation. **Z. Apostolides:** Conceptualization, Writing – review & editing, Supervision.

Declaration of competing interest

The authors declare that they have no known competing financial interests or personal relationships that could have appeared to influence the work reported in this paper.

Data availability

Data will be made available on request.

Acknowledgements

M.T. was partially funded by the University of Pretoria with a post-graduate scholarship and studentship.

Appendix A. Supplementary data

Supplementary data to this article can be found online at https://doi.org/10.1016/j.jep.2023.116377.

References

Adisakwattana, S., Chantarasinlapin, P., Thammarat, H., Yibchok-Anun, S., 2009. A series of cinnamic acid derivatives and their inhibitory activity on intestinal alpha-glucosidase. J. Enzym. Inhib. Med. Chem. 24, 1194–1200. https://doi.org/10.1080/14756360902779326.

Ali, M.S., Jahangir, M., Hussan, S.S., Choudhary, M.I., 2002. Inhibition of alpha-glucosidase by oleanolic acid and its synthetic derivatives. Phytochemistry (Oxf.) 60, 295–299. https://doi.org/10.1016/s0031-9422(02)00104-8.

Alqahtani, A.S., Hidayathulla, S., Rehman, M.T., ElGamal, A.A., Al-Massarani, S., Razmovski-Naumovski, V., Alqahtani, M.S., El Dib, R.A., Al Ajmi, M.F., 2019. Alpha-amylase and alpha-glucosidase enzyme inhibition and antioxidant potential of 3-oxolupenal and katononic acid isolated from *Nuxia oppositifolia*. Biomolecules 10, 1–19. https://doi.org/10.3390/biom10010061.

Barkaoui, M., Katiri, A., Boubakker, H., Msanda, F., 2017. Ethnobotanical survey of medicinal plants used in the traditional treatment of diabetes in Chtouka Ait Baha and Tiznit (Western Anti-Atlas), Morocco. J. Ethnopharmacol. 23, 338–350. https://doi.org/10.1016/j.jep.2017.01.023.

ChemDraw, 2020. PerkinElmer Informatics [Online] Available from: https://informatics.perkinelmer.com.

Chen, D., Wang, Y., Wu, K., Wang, X., 2018. Dual effects of metformin on adipogenic differentiation of 3T3-L1 preadipocyte in AMPK-dependent and independent manners. Int. J. Mol. Sci. 19, 1457. https://doi.org/10.3390/ijms19061547.

Dayarathne, L.A., Ranaweera, S.S., Natraj, P., Rajan, P., Lee, Y.J., Han, C.H., 2021. The effects of naringenin and naringin on the glucose uptake and AMPK phosphorylation in high glucose treated HepG2 cells. J. Vet. Med. 22, 92–104. https://doi.org/10.4142/jvs.2021.22.e92.

Ediriweera, E.R.H.S.S., Ratnasooriya, W.D., 2009. A Review on herbs used in treatment of diabetes mellitus by Sri Lankan ayurvedic and traditional physicians. AYU 30, 373–391 epage=391;aulast=Ediriweera;type=0. https://www.ayujournal.org/article.asp?issn=0974-8520;year=2009;volume=30;issue=4;spa.

Espin, J.C., Gonzalez-Barrio, R., Cerda, B., Lopez-Bote, C., Rey, A.I., Tomas-Barberan, F. A., 2007. Iberian pig as a model to clarify obscure points in the bioavailability and metabolism of ellagitannins in humans. J. Agric. Food Chem. 55, 10476 https://doi.org/10.1021/jf0723864.

Haffner, S.M., 2006. The metabolic syndrome: inflammation, diabetes mellitus, and cardiovascular disease. Am. J. Cardiol. 97, 3–11. https://doi.org/10.1016/j.amjcard.2005.11.010.

Hossain, U., Das, A.K., Ghosh, S., Sil, P.C., 2020. An overview on the role of bioactive α-glucosidase inhibitors in ameliorating diabetic complications. Food Chem. Toxicol. 145, 1–15. https://doi.org/10.1016/j.fct.2020.111738.

Ibrahim, M.A., Serem, J.C., Bester, M.J., Neitz, A.W., Gaspar, A.R.M., 2019. Multiple antidiabetic effects of three α-glucosidase inhibitory peptides, PFP, YPL and YPG: dipeptidyl peptidase-IV inhibition, suppression of lipid accumulation in differentiated 3T3-L1 adipocytes and scavenging activity on methylglyoxal. Int. J. Biol. Macromol. 122, 104–114. https://doi.org/10.1016/j.ijbiomac.2018.10.152.

Khan, F., Bashir, A., Mughairbi, F., 2018. Purple tea composition and inhibitory effect of anthocyanin-rich extract on cancer cell proliferation. Med. Aromatic Plants 7, 1–4. https://doi.org/10.4172/2167-0412.1000322.

Kowalska, K., Olejnik, A., Rychlik, J., Grajek, W., 2014. Cranberries (*Oxycoccus quadripetalus*) inhibit adipogenesis and lipogenesis in 3T3-L1 cells. Food Chem. 148, 246–252. https://doi.org/10.1016/j.foodchem.2013.10.032.

Lin, C., Lin, H., Chang, H., Chuang, L., Hsieh, C., Lu, S., Hung, C., Chang, J., 2022. Prophylactic effects of purple shoot green tea on cytokine immunomodulation through scavenging free radicals and no in lps-stimulated macrophages. Curr. Issues Mol. Biol. 44, 3980–4000. https://doi.org/10.3390/cimb44090273.

Loomba, R., Sanyal, A.J., 2013. The global NAFLD epidemic. Nat. Rev. Gastroenterol. Hepatol. 10, 686–690. https://doi.org/10.1038/nrgastro.2013.171.

Loschwitz, J., Jäckering, A., Keutmann, M., Olagunju, M., Eberle, R.J., Coronado, M.A., Olubiyi, O.O., Strodel, B., 2021. Novel inhibitors of the main protease enzyme of SARS-CoV-2 identified via molecular dynamics simulation-guided in vitro assay. Bioorg. Chem. 111, 104862 https://doi.org/10.1016/j.bioorg.2021.104862.

Mahomoodally, M.F., Mootoosamy, A., Wambugu, S., 2016. Traditional therapies used to manage diabetes and related complications in Mauritius: a comparative ethnoreligious study. Evid Based Complement Alternat Med, 4523828. https://doi.org/10.1155/2016/4523828, 2016.

Mazzei, L., Ciurli, S., Zambelli, B., 2016. Isothermal titration calorimetry to characterize enzymatic reactions. Methods Enzymol. 567, 215–236.

Mehlem, A., Hagberg, C.E., Muhl, L., Eriksson, U., Falkevall, A., 2013. Imaging of neutral lipids by oil red O for analyzing the metabolic status in health and disease. Nat. Protoc. 8, 1149–1154. https://doi.org/10.1038/nprot.2013.055.

Modak, M., Dixit, P., Londhe, J., Ghaskadbi, S., Devasagayam, T.P.A., 2007. Indian herbs and herbal drugs used for the treatment of diabetes. J. Clin. Biochem. Nutr. 40, 163–172. https://doi.org/10.3164/jcbn.40.163.

Perera, A., Ton, S.H., Moorthy, M., Palanisamy, U.D., 2020. The insulin-sensitising properties of the ellagitannin geraniin and its metabolites from *Nephelium lappaceum* rind in 3T3-L1 cells. Int. J. Food Sci. Nutr. 71, 940–953. https://doi.org/10.1080/09637486.2020.1754348.

Poliankyte-Prause, Z., Tolvanen, T.A., Lindfors, S., Dumont, V., Van, M., Wang, H., Dash, S.N., Berg, M., Naams, J.B., Hautala, L.C., Nisen, H., Mirtti, T., Groop, P.H., Wähälä, K., Tienari, J., Lehtonen, S., 2019. Metformin increases glucose uptake and acts renoprotectively by reducing SHIP2 activity. Faseb. J. 33, 2858–2869. https://doi.org/10.1096/fj.201800529RR.

Proença, C., Freitas, M., Ribeiro, D., Oliveira, E.F.T., Sousa, J.L.C., Tomé, S.M., Ramos, M.J., Silva, A.M.S., Fernandes, P.A., Fernandes, E., 2017. α-Glucosidase inhibition by flavonoids: an in vitro and in silico structure-activity relationship study. J. Enzym. Inhib. Med. Chem. 32, 1216–1228. https://doi.org/10.1080/14756366.2017.1368503.

Proença, C., Freitas, M., Ribeiro, D., Tomé, S.M., Oliveira, E.F.T., Viegas, M.F., Araújo, A. N., Ramos, M.J., Silva, A.M.S., Fernandes, P.A., Fernandes, E., 2019. Evaluation of a flavonoids library for inhibition of pancreatic α-amylase towards a structure-activity relationship. J. Enzym. Inhib. Med. Chem. 34, 577–588. https://doi.org/10.1080/14756366.2018.1558221.

Qiu, Z., Zhou, J., Zhang, C., Cheng, Y., Hu, J., Zheng, G., 2018. Antiproliferative effect of urolithin A, the ellagic acid-derived colonic metabolite, on hepatocellular carcinoma HepG2.2.15 cells by targeting Lin28a/let-7a axis. Braz. J. Med. Biol. Res. 51, 7220. https://doi.org/10.1590/1414-431x20187220. – 7228.

Rachid, A., Rabah, D., Farid, L., Zohra, S.F., Houcine, B., Nacera, B., 2012. Ethnopharmacological survey of medicinal plants used in the traditional treatment of diabetes mellitus in the North Western and South Western Algeria. J. Med. Plants Res. 6, 2041–2050. https://doi.org/10.5897/JMPR11.1796.

Regufe, V.M.G., Pinto, C., Perez, P., 2020. Metabolic syndrome in type 2 diabetic patients: a review of current evidence. Porto Biomed J 5, 101–107. https://doi.org/10.1097/j.pbj.0000000000000101.

Sánchez-Pérez, A., Andrés, M., Peña-García, J., den-Haan, H., Bekas, N., Katsikoudi, A., Tzakos, A.G., Sánchez-Pérez, H., 2015. DIA-DB: a web-accessible database for the prediction of diabetes drugs. In: Ortuño, F., Rojas, I. (Eds.), Bioinformatics and Biomedical Engineering. IWBBIO 2015. Lecture Notes in Computer Science. Springer Cham., New York, pp. 655–663. https://doi.org/10.1007/978-3-319-16480-9_63.

Schrodinger, L.L.C., 2021. *Maestro*. 2022-2 [Online] Available from: https://www.schrodinger.com.

Sun, H., Saeedi, P., Karuranga, S., Pinkepank, M., Ogurtsova, K., Duncan, B.B., Stein, C., Basit, A., Chan, J.C.N., Mbanya, J.C., Pavkov, M.E., Ramachandaran, A., Wild, S.H., James, S., Herman, W.H., Zhang, P., Bommer, C., Kuo, S., Boyko, E.J., Magliano, D. J., 2022. IDF Diabetes Atlas: global, regional and country-level diabetes prevalence estimates for 2021 and projections for 2045. Diabetes Res. Clin. Pract. 183, 109119 https://doi.org/10.1016/j.diabres.2021.109119.

Sun, J., Ren, J., Hu, X., Hou, Y., Yang, Y., 2021. Therapeutic effects of Chinese herbal medicines and their extracts on diabetes. Biomed. Pharmacother. 142, 111977 https://doi.org/10.1016/j.biopha.2021.111977.

Tilg, H., Moschen, A.R., Roden, M., 2017. NAFLD and diabetes mellitus. Nat. Rev. Gastroenterol. Hepatol. 14, 32–42. https://doi.org/10.1038/nrgastro.2016.147.

Tshiyoyo, K.S., Bester, M.J., Serem, J.C., Apostolides, Z., 2022. In-silico reverse docking and in-vitro studies identified curcumin, 18α-glycyrrhetinic acid, rosmarinic acid, and quercetin as inhibitors of α-glucosidase and pancreatic α-amylase and lipid accumulation in HepG2 cells, important type 2 diabetes targets. J. Mol. Struct. 1266, 1–10. https://doi.org/10.1016/j.molstruc.2022.133492.

Vichai, V., Kirtikara, K., 2006. Sulforhodamine B colourimetric assay for cytotoxicity screening. Nat. Protoc. 1, 1112–1116. https://doi.org/10.1038/nprot.2006.179.

Villalba, K.J.O., Barka, F.V., Pasos, C.V., Rodriguez, P.E., 2019. Food ellagitannins: structure, metabolomic fate, and biological properties. In: Aires, A. (Ed.), Tannins - Structural Properties, Biological Properties and Current Knowledge. IntechOpen, London. https://doi.org/10.5772/intechopen.86420.

Wang, Y., Qiu, Z., Zhou, B., Liu, C., Ruan, J., Yan, Q., Liao, J., Zhu, F., 2015. In vitro antiproliferative and antioxidant effects of urolithin A, the colonic metabolite of ellagic acid, on hepatocellular carcinomas HepG2 cells. Toxicol. Vitro 29, 1107–1115. https://doi.org/10.1016/j.tiv.2015.04.008.

Yang, X., Kong, F., 2016. Evaluation of the in vitro α-glucosidase inhibitory activity of green tea polyphenols and different tea types. J. Sci. Food Agric. 96, 777–782. https://doi.org/10.1002/jsfa.7147.

Yang, X., Tomas-Barberan, F.A., 2019. Tea Is a significant dietary source of ellagitannins and ellagic acid. J. Agric. Food Chem. 67, 5394–5404. https://doi.org/10.1021/acs.jafc.8b05010.

Yu, X., Xiao, J., Chen, S., Yu, Y., Ma, J., Lin, Y., Li, R., Lin, J., Fu, Z., Zhou, Q., Chao, Q., Chen, L., Yang, Z., Liu, R., 2020. Metabolite signatures of diverse Camellia sinensis tea populations. Nat. Commun. 11, 5586–5600. https://doi.org/10.1038/s41467-020-19441-1.

Zhang, Y., Aisker, G., Dong, H., Halemahebai, G., Zhang, Y., Tian, L., 2021. Urolithin A suppresses glucolipotoxicity-induced ER stress and TXNIP/NLRP3/IL-1β inflammation signal in pancreatic β cells by regulating AMPK and autophagy. Phytomedicine 93. https://doi.org/10.1016/j.phymed.2021.153741.